Subtype-specific Modulation of Acid-sensing Ion Channel (ASIC) Function by 2-Guanidine-4-methylquinazoline*[S]

Omar Alijevic and Stephan Kellenberger[1]

From the Department of Pharmacology and Toxicology, University of Lausanne, 1005 Lausanne, Switzerland

Background: The small molecule GMQ opens ASIC3 channels by an unknown mechanism.
Results: GMQ alters pH-dependent gating in all ASICs and amplifies an existing sustained current in ASIC3.
Conclusion: The consequences of GMQ binding on channel function are ASIC subtype-dependent.
Significance: This study describes the complex effects of a novel class of small molecules on ASIC function.

Acid-sensing ion channels (ASICs) are neuronal Na$^+$-selective channels that are transiently activated by extracellular acidification. ASICs are involved in fear and anxiety, learning, neurodegeneration after ischemic stroke, and pain sensation. The small molecule 2-guanidine-4-methylquinazoline (GMQ) was recently shown to open ASIC3 at physiological pH. We have investigated the mechanisms underlying this effect and the possibility that GMQ may alter the function of other ASICs besides ASIC3. GMQ shifts the pH dependence of activation to more acidic pH in ASIC1a and ASIC1b, whereas in ASIC3 this shift goes in the opposite direction and is accompanied by a decrease in its steepness. GMQ also induces an acidic shift of the pH dependence of inactivation of ASIC1a, -1b, -2a, and -3. As a consequence, the activation and inactivation curves of ASIC3 but not other ASICs overlap in the presence of GMQ at pH 7.4, thereby creating a window current. At concentrations >1 mM, GMQ decreases maximal peak currents by reducing the unitary current amplitude. Mutation of residue Glu-79 in the palm domain of ASIC3, previously shown to be critical for channel opening by GMQ, disrupted the GMQ effects on inactivation but not activation. This suggests that this residue is involved in the consequences of GMQ binding rather than in the binding interaction itself. This study describes the mechanisms underlying the effects of a novel class of ligands that modulate the function of all ASICs as well as activate ASIC3 at physiological pH.

Acid-sensing ion channels (ASICs)[2] are members of the epithelial Na$^+$ channel/degenerin family of ion channels (1). They are expressed in the nervous system where they form Na$^+$-selective channels that are activated by extracellular acidifica-

tion (2). ASICs in the central nervous system were shown to play roles in the expression of fear, learning, and neurodegeneration after ischemia (3–5). ASICs of the peripheral nervous system are involved in both pain sensation and mechanosensation (6–8). Six homologous ASIC subunits have been cloned. In the recently published crystal structure of ASIC1, the channel is composed of three subunits (9, 10). ASIC1a, -1b, -2a, and -3 can form homo- or heteromultimeric channels whose pH dependence and kinetics depend on the subunit composition. ASIC2b is a modulatory subunit that can participate in the formation of heteromultimeric channels (11). For ASIC4, no channel function has been found so far (12).

For a long time, protons were the only known activators of ASICs. The small molecule 2-guanidine-4-methylquinazoline (GMQ) and related substances have recently been shown to open ASIC3 and constitute the first known nonproton ASIC activators (13). It was shown that mutations in the highly conserved lower palm domain disrupt the activation by GMQ and/or change the EC$_{50}$ of activation, suggesting that the lower palm domain is critically involved in ASIC3 activation by GMQ (13, 14). At pH 7.4, GMQ opens only ASIC3 but no other ASICs (13). Given the high sequence homology of the lower palm domain between different ASIC subunits, we hypothesized that GMQ may bind to all ASICs and affect their function. The aim of the study was to determine by which mechanisms GMQ opens ASIC3 at pH 7.4 and to characterize its possible effects on other ASICs. We show that GMQ shifts the pH dependence of activation and steady-state inactivation of ASIC1a, -1b, -2a, and -3 but that these shifts allow channel activation at the physiological pH 7.4 only in ASIC3.

EXPERIMENTAL PROCEDURES

Site-directed Mutagenesis and Expression in Xenopus Oocytes—Point mutations were introduced by QuikChange (Stratagene). Mutations were verified by sequencing (Synergene Biotech, Zurich, Switzerland). For expression in *Xenopus* oocytes, the ASIC1a cDNA (15) was cloned into a vector containing 5′- and 3′-untranslated sequences of *Xenopus* β-globin. Complementary RNAs were synthesized *in vitro*. Oocytes were surgically removed from the ovarian tissue of female *Xenopus laevis* that had been anesthetized by immersion in 2 g/liter MS-222 (Sandoz, Basel, Switzerland). The oocytes were defolliculated, and healthy stage V and VI oocytes were isolated and

[2] The abbreviations used are: ASIC, acid-sensing ion channel; ctrl, control; GMQ, 2-guanidine-4-methylquinazoline; MTSET, 2-trimethylammonium ethyl methanethiosulfonate; n_H, Hill coefficient; pH$_{50}$, pH of half-maximal activation; pHIn$_{50}$, pH of half-maximal inactivation; SSIN, steady-state inactivation.

pressure-injected with 50–100 nl of cRNA solution. Oocytes were kept in modified Barth solution during the expression phase. All experimental procedures on *X. laevis* were realized according to the Swiss federal law on animal welfare approved by the committee on animal experimentation of the Canton de Vaud.

Recombinant Expression of ASICs in CHO Cells—Previously described Chinese hamster ovary (CHO) cell lines stably expressing human ASIC1a, rat ASIC1b, human ASIC2a, and rat ASIC3 were used in the present experiments (16). For transient transfections (single-channel experiments and mutants), ASIC cDNA in the expression vector pCDNA3.1 (Invitrogen) or pCI (Promega) together with a green fluorescent protein construct was used to transfect CHO cells using Lipofectamine 2000 (Invitrogen). For single-channel experiments, different amounts of ASIC cDNA were transfected to obtain the desired low channel density. Cells were grown in DMEM/F-12 (Invitrogen) supplemented with 3.6% FCS and 1% penicillin/streptomycin.

Electrophysiological Measurements from CHO Cells—Electrophysiological measurements were carried out in the whole cell or excised outside-out configuration of the patch clamp technique with an EPC9 patch clamp amplifier (HEKA Electronics, Lambrecht, Germany). Data acquisition was done with HEKA Patchmaster software. The sampling interval was set to 1 ms, and filtering was set to 3 kHz in whole-cell experiments and 0.1 ms and 3 kHz in single-channel experiments. Fast solution exchange was achieved using the computer-controlled electrovalve assembly EVH-9 (Biologic, Claix, France) and the MPRE8 perfusion head (Cell MicroControls, Norfolk, VA). Pipettes were pulled from borosilicate glass (World Precision Instruments, Stevenage, UK) and had resistances between 2 and 5 megaohms for whole-cell recording (thin-walled glass) and 5–12 megaohms for single-channel recording (thick-walled glass) when filled with the pipette solution. Series resistance compensation was set to 70–95% in all whole-cell experiments. Experiments were performed at a holding potential of −60 mV.

Pipette solutions contained 90 mM potassium gluconate, 10 mM NaCl, 10 mM KCl, 1 mM $MgCl_2$, 60 mM Hepes, 10 mM EGTA. For single-channel recording the pipette solution contained 90 mM CsOH, 90 mM gluconic acid, 10 mM KCl, 10 mM NaCl, 1 mM $MgCl_2$, 60 mM Hepes. The pH of all solutions was adjusted to pH 7.3 with NaOH. Extracellular solutions contained 140 mM NaCl, 4 mM KCl, 2 mM $CaCl_2$, 1 mM $MgCl_2$, 10 mM Hepes, 10 mM MES, 10 mM glucose; pH was adjusted to the desired value using NaOH/HCl.

Analysis was carried out with Fitmaster (HEKA Electronics) for whole-cell data and with TAC (Bruxton, Seattle, WA) for single-channel recordings. For single-channel analysis, data were digitally low pass-filtered at 100 Hz. Open and closed events were carefully checked visually before being accepted. Amplitude histograms of single-channel openings were generated using TACFit (Bruxton). Single-channel amplitudes were estimated from Gaussian fits of the amplitude histograms.

Electrophysiological Measurements from Xenopus Oocytes—Electrophysiological measurements were performed at 18–30 h after cRNA injection. Macroscopic currents were recorded using the two-electrode voltage clamp technique at a holding potential of −60 mV. Currents were recorded using a Dagan TEV-200 amplifier (Minneapolis, MN) equipped with two bath electrodes and analyzed with the pCLAMP data acquisition package (Molecular Devices, Sunnyvale, CA). The standard bath solution contained 110 mM NaCl, 2.0 mM $CaCl_2$, 10 mM Hepes-NaOH (or MES-NaOH for pH <6.8), and pH was adjusted by NaOH to the values indicated. Oocytes were placed in a recording chamber (500 μl) and perfused by gravity at a rate of 5–15 ml/min.

Chemicals—GMQ, a product of the Sigma-Aldrich rare chemical library, was obtained from Sigma. A sample was analyzed by liquid chromatography coupled to mass spectrometry, confirming the identity and indicating a purity of 98.5% (mass spectrometry service at the Ecole Polytechnique Fédérale de Lausanne). GMQ solutions were made fresh every day. MTSET was from Toronto Research (Toronto, Canada). Other chemicals were obtained from Acros Organics (Geel, Belgium), Applichem (Darmstadt, Germany), Sigma, or Fluka (Buchs, Switzerland).

Analysis and Statistics—The pH activation curves were fitted using the Hill equation: $I = I_{max}/[1 + (10^{-pH50}/10^{-pH})^{nH}]$ where I_{max} is the maximal current, pH_{50} is the pH at which half of the maximal current is measured, and n_H is the Hill coefficient. Steady-state inactivation (SSIN) curves were fitted by an analogous equation. Data are presented as mean ± S.E. Differences between the absence and presence of GMQ were analyzed using Student's *t* test.

RESULTS

GMQ Shifts the pH Dependence of ASIC3 and Induces a Sustained Current—In CHO cells stably expressing ASIC3, GMQ application generated a sustained inward current at pH 7.4 as reported previously (13) (Fig. 1*A*). At 1 mM GMQ and pH 7.4, the GMQ-induced current amplitude showed some variability and corresponded to 4.4 ± 14.7% of the pH 5-induced peak amplitude in the same cell (*n* = 10), which is lower than the value described previously (13). To investigate the possible mechanisms by which GMQ opens ASIC3 at pH 7.4, the pH dependence of ASIC3 under control conditions and in the presence of 1 mM GMQ was determined. Representative current traces illustrate that the principal effect of GMQ is the induction of a sustained current with maximal amplitudes in the pH range 6.5–7 (Fig. 1*A*) as reported previously (13). The current amplitudes of this combined transient/sustained current are plotted as a function of pH in Fig. 1*B*, which shows a shift of the activation curve to more alkaline values in the presence of GMQ. Interestingly, the change in the activation curve occurs in the pH range at which the sustained current is greatest (Fig. 1, *A* and *B*), suggesting that the appearance of the sustained current may introduce this shift. The sustained current at pH 7.0 and 0.5 mM GMQ was inhibited by amiloride with an IC_{50} of 99 ± 24 μM (*n* = 5; supplemental Fig. S1A). In the absence of GMQ, amiloride activated ASIC3 at pH 7 as reported previously (17) (supplemental Fig. S1B).

Because GMQ induces a sustained current, it does not only open ASIC3 but must also interfere with inactivation. To quantify the effect of GMQ on inactivation, the pH dependence of SSIN was measured. SSIN represents the transition from the
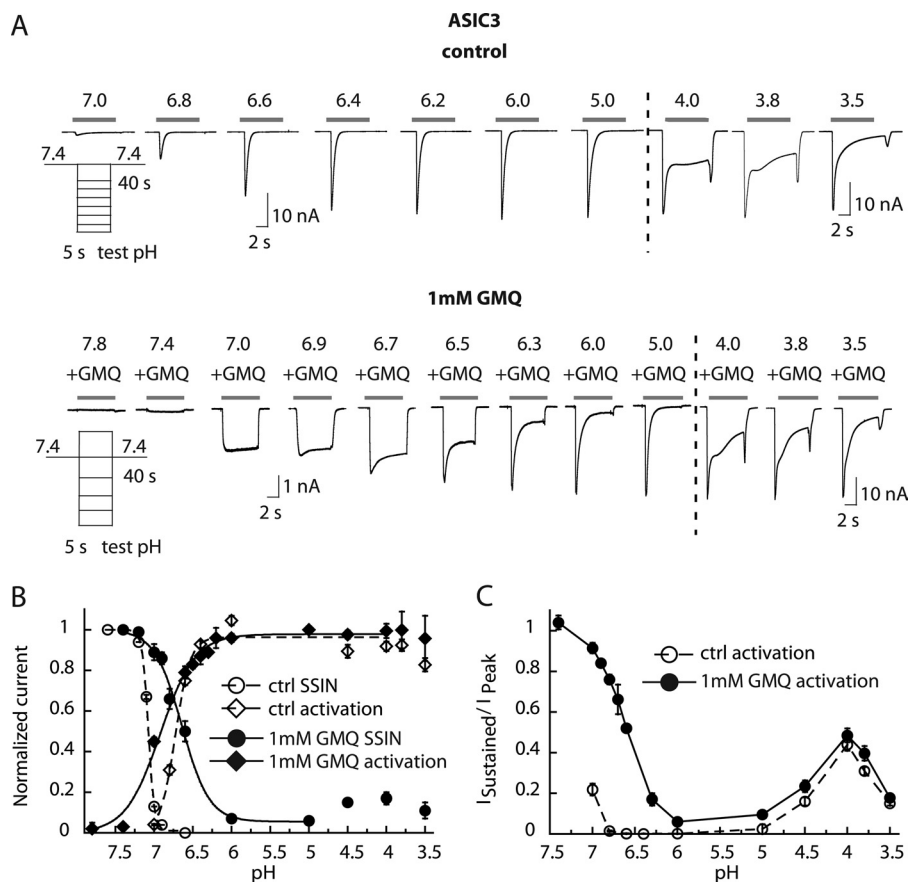
FIGURE 1. **GMQ changes the pH dependence of ASIC3 gating and impairs inactivation.** Currents were measured by whole-cell patch clamp at a holding potential of −60 mV from CHO cells stably expressing ASIC3. *A*, current traces of ASIC3 in the absence (*top*) or presence (*bottom*) of 1 mM GMQ. Traces obtained at pH 4.0–3.5 (*right panel*) are of a different experiment. *B*, ASIC3 was activated by switching from a conditioning pH of 7.4 to various acidic test pH values for 5 s once every 40 s. For the activation curve, the normalized current response is plotted as a function of the stimulation pH for control condition (*open symbols*) or in the presence of 1 mM GMQ in the acidic test solutions (*filled symbols*) ($n = 4–11$). For SSIN, a conditioning pH in the range of pH 7.6–6.5 was applied for 60 s, and the fraction of non-inactivated channels was measured by applying pH 6 for 5 s. This protocol was repeated with increasingly acidic conditioning pH values. In the SSIN curve, normalized currents are plotted as a function of the conditioning pH for the control condition (*open symbols*) and in the presence of 1 mM GMQ in the conditioning solution (*filled symbols*) ($n = 4–5$). For fit parameters, see Table 1. *C*, pH dependence of the sustained ASIC3 current fraction in the absence or presence of 1 mM GMQ. The ratio of sustained/peak current amplitude is plotted ($n = 4–8$). *Error bars* represent S.E.

closed to the inactivated state during prolonged exposure to moderately acidic pH. ASIC3 channels were exposed to conditioning solutions of different pH values for 60 s followed by stimulation by pH 6. The normalized peak current amplitude in the absence and presence of 1 mM GMQ in the conditioning solution is plotted as a function of the conditioning pH in Fig. 1*B*. The SSIN curve is shifted to more acidic pH and is less steep in the presence of GMQ, leading to an overlap between the activation and the SSIN curve. In the pH window of the overlap, channels are opened but only partially inactivated, leading to the observed sustained current. By generating this window current, GMQ can thus open ASIC3 at pH 7.4. ASIC3 has been known to mediate a substantial sustained current at very acidic pH as well as a small sustained current at around pH 7 (18, 19). GMQ does not affect the sustained current fraction at pH <5; however, it massively amplifies the sustained current component in the range above pH 6 (Fig. 1, *A* and *C*).

GMQ Modulates the Function of Subtypes Other than ASIC3—It was shown that GMQ does not open ASIC1a, -1b, or -2a at pH 7.4 (13). Because the highly conserved lower palm region was shown to be important for the actions of GMQ (13, 14), we hypothesized that GMQ may also affect the function of

other ASICs but without activating these channels at pH 7.4. To test this hypothesis, activation and SSIN curves were recorded from ASIC1a- and ASIC1b-expressing cells in the presence and absence of 1 mM GMQ. 5 mM GMQ was used with ASIC2a because on this subtype 1 mM GMQ had no significant effect. Fig. 2*A* shows representative current traces from ASIC1a-expressing cells in the absence and presence of 1 mM GMQ. In these ASIC subtypes, GMQ shifted the pH dependence of SSIN to more acidic values (Fig. 2, *B–D*; $p < 0.05$) as it also does in ASIC3 (Table 1 and Fig. 1*B*). GMQ shifted the pH dependence of activation of ASIC1a and -1b to more acidic values (Fig. 2, *B* and *C*, and Table 1; $p < 0.05$), thus in the opposite direction of its effect on ASIC3. The activation curve of ASIC2a is not affected by GMQ (Fig. 2*D* and Table 1). None of these three ASIC subtypes showed an overlap in their activation and SSIN curves at pH 7.4 in the presence of GMQ, explaining the reported absence of channel activation by GMQ (13). For ASIC1b, such an overlap was seen in the presence of 1 mM GMQ at pH 6.3–6.6, suggesting that in the presence of GMQ or related physiological analogs pH 6.3–6.6 should induce a sustained current. Indeed, a sustained current was observed at pH 6.4 (supplemental Fig. S2). The amplitude of this current at the
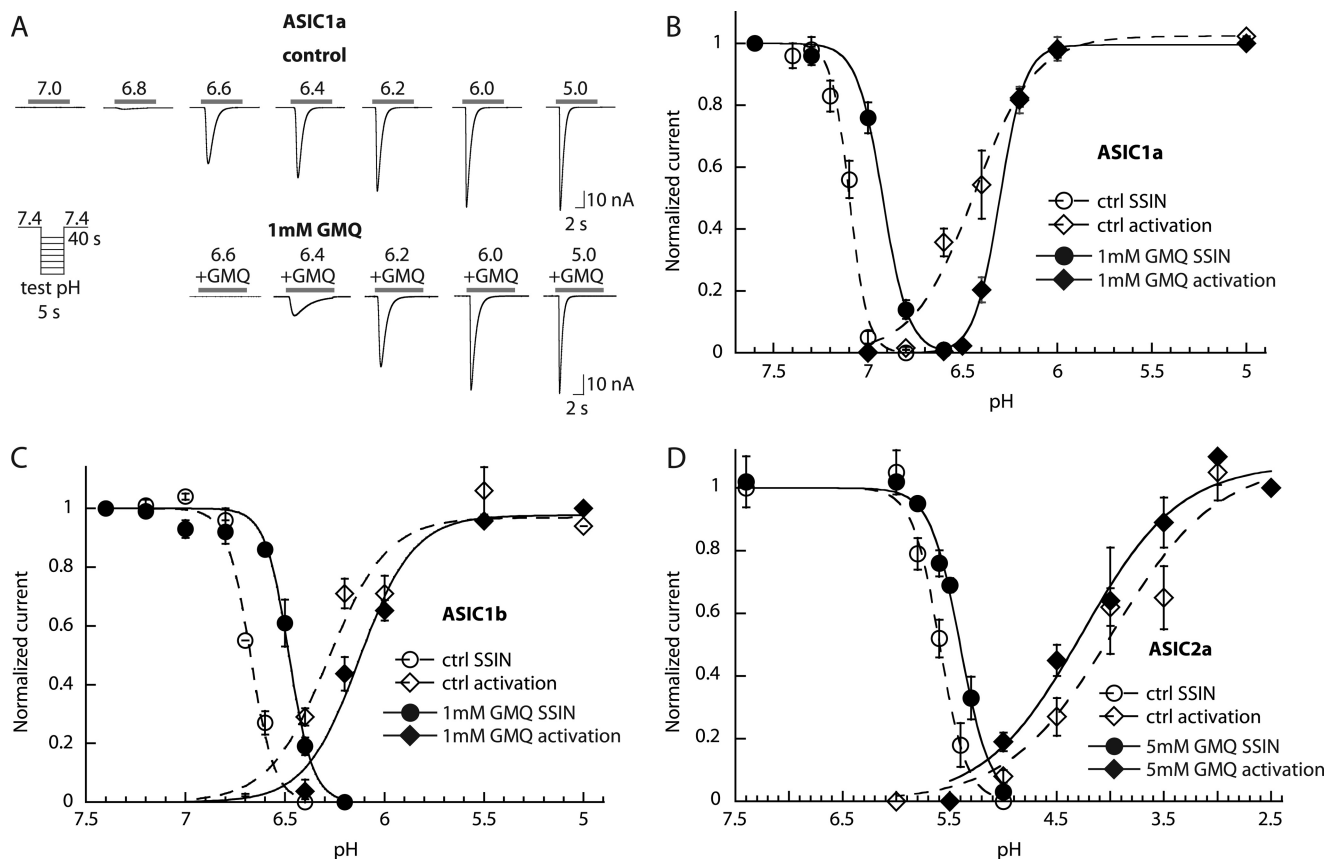
FIGURE 2. **GMQ shifts the pH dependence of ASIC1a, -1b, and -2a.** The currents were measured by whole-cell voltage clamp to -60 mV from CHO cells stably expressing the ASIC homomultimers (ASIC1a, -1b, and -2a). *A*, current traces of representative activation curves of ASIC1a in the absence (*top*) or presence (*bottom*) of 1 mM GMQ. Activation and SSIN curves were measured as described in the text and in the legend to Fig. 1 and are plotted in *B* for ASIC1a ($n = 5–6$), *C* for ASIC1b ($n = 3–12$), and *D* for ASIC2a ($n = 3–6$). *Open symbols* correspond to data obtained in control conditions, and *filled symbols* correspond to data obtained with 1 mM GMQ (5 mM GMQ for ASIC2a) in the acidic test solutions for activation curves and conditioning solutions for SSIN curves, respectively. *Error bars* represent S.E.

TABLE 1

pH dependence of ASIC gating in the presence and absence of GMQ

GMQ, in the presence of 1 mM GMQ for ASIC1a, -1b, and -3 or 5 mM GMQ for ASIC2a. The extracellular Ca^{2+} concentration in these experiments was 2 mM.

	ASIC1a	ASIC1b	ASIC2a	ASIC3
Activation				
pH_{50} control	6.49 ± 0.02	6.27 ± 0.02	3.95 ± 0.17	6.71 ± 0.01
pH_{50} GMQ	6.30 ± 0.02^a	6.14 ± 0.02^b	4.17 ± 0.14	6.94 ± 0.03^a
n_H control	3.42 ± 0.34	3.18 ± 0.37	1.09 ± 0.14	4.05 ± 0.06
n_H GMQ	6.91 ± 0.49^a	3.93 ± 0.30	1.13 ± 0.13^c	2.27 ± 0.24^a
SSIN				
$pHIn_{50}$ control	7.11 ± 0.01	6.66 ± 0.01	5.63 ± 0.03	7.07 ± 0.00
$pHIn_{50}$ GMQ	6.92 ± 0.02^a	6.48 ± 0.01^a	5.42 ± 0.04^c	6.59 ± 0.00^a
n_H control	9.23 ± 2.39	8.57 ± 0.51	3.18 ± 0.10	10.75 ± 0.19
n_H GMQ	6.57 ± 0.61	8.04 ± 0.74	3.08 ± 0.29	2.05 ± 0.21^a
n	5–6	3–12	3–6	4–11

[a] Different from control, $p < 0.001$.
[b] Different from control, $p < 0.01$.
[c] Different from control, $p < 0.05$.

end of a 5-s exposure to pH 6.4 was $9 \pm 1\%$ of the pH 5-induced current amplitude in the presence of 1 mM GMQ in the same cell ($n = 9$). The acidic shift of the activation curves of ASIC1a and -1b indicates that in these channels exposure to GMQ in the pH range ~6.8–6.2 decreases the current amplitude.

Concentration Dependence of ASIC Modulation by GMQ— To determine the concentration dependence of the action of GMQ on the different ASIC subtypes, activation curves in the presence of increasing concentrations of GMQ were recorded for ASIC1a, -1b, and -3 as shown in Fig. 3, *A–C*. GMQ shifts the

activation curves of ASIC1a and -1b in a concentration-dependent manner to more acidic values (Fig. 3, *A* and *B*). Fig. 3*D* plots the GMQ-induced shift of the ASIC1a pH_{50}. The EC_{50} for the pH_{50} shift was 1.97 ± 0.29 mM ($n = 4–6$). In ASIC1b, the shifts were much smaller. Therefore, the GMQ concentration *versus* pH_{50} relationship could not be accurately fitted. Its EC_{50} is in the range of 1–3 mM ($n = 4–6$; supplemental Fig. S3A). Activation curves obtained with ASIC3 in the presence of different concentrations of GMQ are shown in Fig. 3*C*. Increasing the GMQ concentration induced small changes in the ASIC3
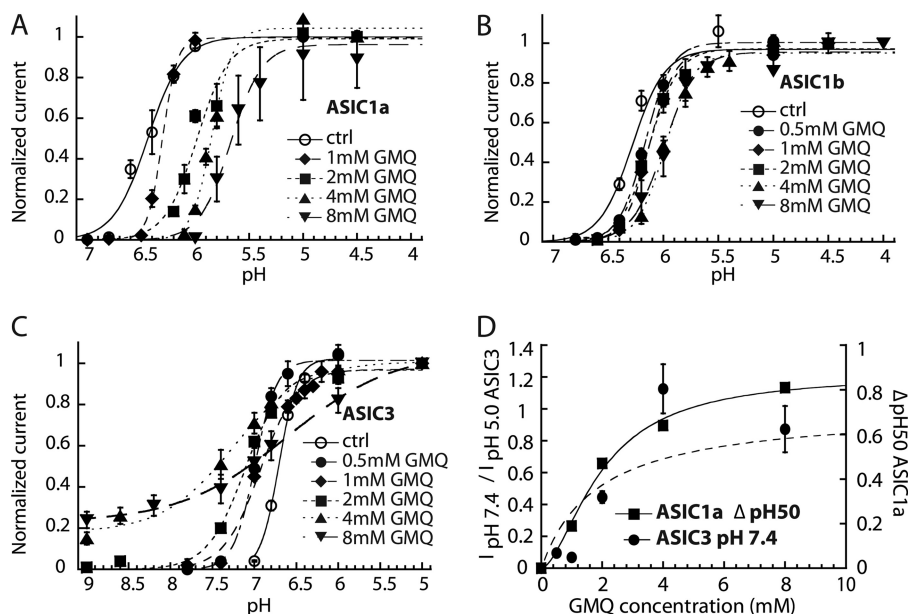
FIGURE 3. **Concentration dependence of the effects of GMQ on ASIC gating.** Currents were measured by whole-cell voltage clamp to −60 mV from CHO cells stably expressing the ASIC homomultimers (ASIC1a, -1b, and -3). *A–C*, activation curves obtained in the presence of the indicated GMQ concentrations in the stimulation solution for ASIC1a (*A*), ASIC1b (*B*), and ASIC3 (*C*). The *lines* represent fits to the Hill equation (see "Experimental Procedures"). *D*, the amplitude of the GMQ-induced ASIC3 current at pH 7.4 normalized to the pH 5-induced current amplitude and the shift in pH_{50} of ASIC1a are plotted as a function of the GMQ concentration. Fit parameters are for ASIC3: EC_{50}, 1.83 ± 0. 97 mM (*n* = 4–6). For ASIC1a, the EC_{50} of the GMQ-induced shift in pH_{50}, obtained from the fit shown as a *solid line*, was 1.97 ± 0.29 mM (*n* = 4–6). *Error bars* represent S.E.

pH_{50} but mainly reduced the steepness of the activation curve, and at concentrations of ≥4 mM, GMQ opened ASIC3 at pH values as alkaline as pH 9. GMQ activated ASIC3 at pH 7.4 with an EC_{50} of 1.83 ± 0. 97 mM (*n* = 4–6; Fig. 3*D*). The EC_{50} at which the n_H value (*i.e.* the steepness) of the pH activation curve decreases was 1.59 ± 0.70 mM (*n* = 4–6; supplemental Fig. S3*B*).

High Concentrations of GMQ Block the ASIC Pore—At a concentration of 1 mM, GMQ only slightly changed the maximal peak current of ASIC1a and ASIC3 as illustrated by the I_{GMQ}/I_{ctrl} ratio of 0.76 ± 0.08 for ASIC1a and 0.87 ± 0.05 for ASIC3 (*n* = 4–5) measured at the most acidic pH tested. In contrast, ASIC1b was substantially inhibited by 1 mM GMQ as reflected by the I_{GMQ}/I_{ctrl} ratio of 0.53 ± 0.04 at pH 4.5 (*n* = 8; Fig. 4*A*). At higher concentrations, GMQ also inhibited the maximal peak current amplitude of ASIC1a and -3 as shown in Fig. 4*A*. The IC_{50} value of inhibition was 3.24 ± 0.81 mM for ASIC1a (*n* = 5), 1.52 ± 0.44 mM for ASIC1b (*n* = 4), and 6.74 ± 0.83 mM for ASIC3 (*n* = 5). To obtain information on the possible nature of this current inhibition, we measured currents from excised outside-out patches containing ASIC1a or ASIC3 at various channel densities. In macropatches, we first confirmed that on ASIC1a 2 mM GMQ inhibited the current amplitude by ~40% (Fig. 4*B*, *left panel*) as it did in the whole-cell mode. A typical trace shows that 2 mM GMQ blocked ~85% of the ASIC3 current in macropatches (Fig. 4*B*, *right panel*). The concentration dependence of ASIC3 block is therefore shifted to lower GMQ concentrations in macropatches as compared with whole-cell measurements (Fig. 4*A*). Even at 1 mM GMQ, unitary ASIC3 currents were difficult to resolve. Therefore, single-channel experiments with ASIC3 were carried out at 0.5 mM GMQ. Unitary ASIC1a and ASIC3 current amplitudes were measured from patches containing a small number of channels (Fig. 4*C*).

Amplitude histograms are shown in Fig. 4*D*. The unitary current amplitude at −60 mV for ASIC1a was 1.46 ± 0.30 pA (108 events) under control conditions and 0.69 ± 0.19 pA (93 events) in the presence of 2 mM GMQ. For ASIC3, the unitary current amplitude was 1.57 ± 0.29 pA (100 events) under control conditions and 0.97 ± 0.21 pA (179 events) in the presence of 0.5 mM GMQ. These experiments indicate that GMQ reduces in both ASIC1a and ASIC3 the unitary current amplitude, which is most likely due to binding in the pore.

Dependence of GMQ Effects on Lower Palm Residues in ASIC3—In ASIC3, mutations of Glu-79 and Glu-423 decreased GMQ-induced current amplitudes at pH 7.4 and/or increased the EC_{50} of GMQ for ASIC opening (13, 14). Thus, we tested how these mutations affect the pH dependence of ASIC3. The E79A mutation shifts the pH of half-maximal inactivation ($pHIn_{50}$) to more alkaline values as reported previously (20). GMQ at 1 mM did not significantly change the SSIN pH dependence of this mutant in strong contrast to its effect on ASIC3 WT (compare Fig. 5*A* with Fig. 1*B*). The activation pH dependence was measured from a conditioning pH of 8.8 to compensate for the alkaline shift of SSIN induced by this mutation, thereby allowing the current measurement. The effect of GMQ on activation was qualitatively similar to that in ASIC3 WT, *i.e.* a strong decrease in the steepness of the activation curve, allowing a transient channel activation by pH 7.4 and a sustained activation by pH 8 in the presence of GMQ (Fig. 5*A*). Obviously, GMQ is still able to bind to this mutant channel, and although its effect on inactivation is disrupted, it still induces a sustained current and shifts the activation curve to more alkaline values. In the E423A mutant, GMQ did not change the pH dependence of the SSIN or the pH dependence of activation, confirming the previously reported critical role of this residue for the functional effect of GMQ (Fig. 5*B*). Combination of the
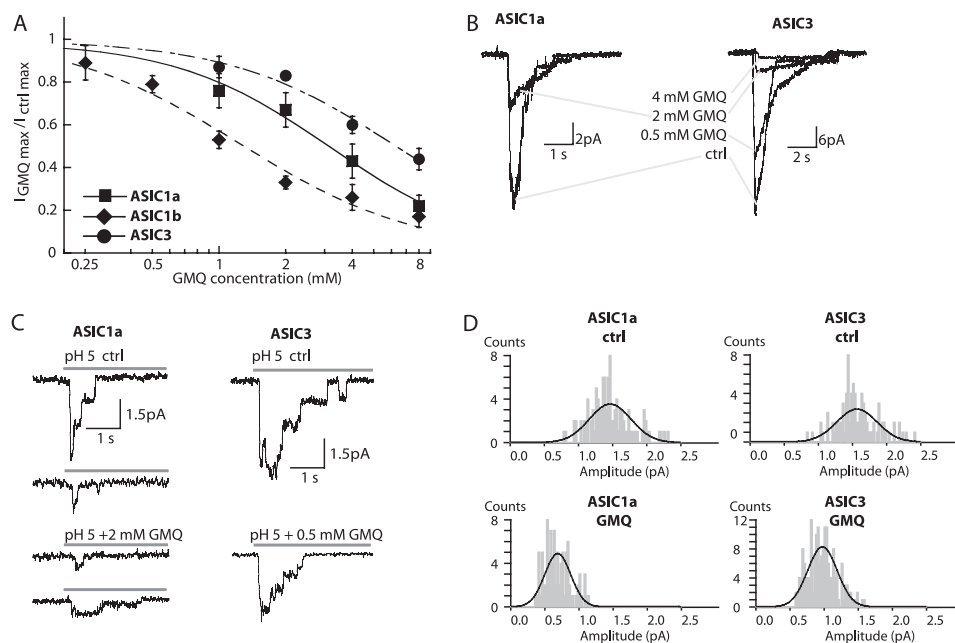
FIGURE 4. **Pore block by GMQ.** *A*, the maximal peak current amplitude of ASIC1a (measured at pH 4.5), ASIC1b (pH 4.5), and ASIC3 (pH 5.0) is plotted as a function of GMQ concentration ($n = 3$–6). Data are from whole-cell voltage clamp to -60 mV. IC_{50} values determined from the fit are indicated in the text. *B–D*, data are from excised outside-out patches voltage-clamped to -60 mV from CHO cells except where noted. *B*, current traces of ASIC1a (*left panel*; from *Xenopus* oocytes) and ASIC3 (*right panel*) from patches containing a large number of channels measured at pH 5.0 in the absence or presence of different concentrations of GMQ. *C*, current traces of ASIC1a (*left panel*) and ASIC3 (*right panel*) from patches with small numbers of channels measured at pH 5.0 in the absence (*upper panels*) or presence (*lower panels*) of 2 mM GMQ (ASIC1a) or 0.5 mM GMQ (ASIC3). In these experiments, GMQ perfusion was started briefly (3 s) before switching to the acidic solutions. *D*, amplitude histograms. Single-channel amplitudes were determined from Gaussian fits of amplitude histograms derived from different patches (see "Experimental Procedures"). *Error bars* represent S.E.

two mutations shifted the pH_{50} to more acidic values. GMQ induced only a tiny alkaline shift in the activation curve of this double mutant (supplemental Fig. S4).

Partial Disruption of GMQ Effects by a Mutation in the ASIC1a Palm Domain—The ASIC3 residues Glu-79 and Glu-423 are located in the lower palm domain that is highly conserved between ASIC subunits. The position of the homologous residues in ASIC1a, Glu-79 and Glu-418, is shown in the structural model of ASIC1a in Fig. 6A (9). Glu-79 and Glu-418 are located close to each other on two adjacent β-strands. Their side chains point toward the central cavity. Fig. 6B illustrates the high sequence conservation of this region and indicates the position of these two residues.

To test the involvement of the lower palm domain of ASIC1a in the effects of GMQ, the ASIC1a residues Glu-79 and Glu-418 were mutated, and mutant channels were expressed in *Xenopus* oocytes to measure channel function by two-electrode voltage clamp. In ASIC1a WT, 1 mM GMQ induced a robust acidic shift in the pH dependence of activation and SSIN (Fig. 2B). The mutations ASIC1a-E79C and -E418C both shift the SSIN curves to more alkaline values with regard to wild type (Fig. 6, C and D). We have shown previously that substitution of Glu-418 by small, hydrophobic residues induces an alkaline shift in the pH dependence of SSIN, although larger and more hydrophilic residues at this position induce an acidic shift (21). The lower palm domain likely undergoes conformational changes that are facilitated by small hydrophobic residues and hindered by large hydrophilic residues at positions Glu-79 and Glu-418 (20, 21). In both mutants, 1 mM GMQ increased the steepness of the activation curve (Fig. 6, C and D) as observed in WT ASIC1a

(Fig. 2B). In the ASIC1a-E418C mutant, the activation curve was shifted by GMQ as in WT ASIC1a. In ASIC1a-E79C, this shift was not observed, indicating that the mutation partially prevents the effect of GMQ on activation. However, in both mutants, GMQ induced an acidic shift in SSIN, indicating that the modulatory effect of GMQ on SSIN was retained (Fig. 6, C and D).

We constructed ASIC1a channels in which both Glu-418 and Glu-79 were mutated. To avoid possible cross-linking, the residues were mutated to Ala instead of Cys. The E79A/E418A double mutant displayed a sustained current without a transient component and was inactivated only partially even at a pH as acidic as pH 3.5 (remaining current of $86 \pm 7\%$ ($n = 3$) of control current after 1-min conditioning at pH 3.5). Therefore, it was not possible to reliably measure a potential effect of GMQ on SSIN. The activation curve of this double mutant was not affected by 1 mM GMQ (Fig. 6F). This further confirms the involvement of the lower palm region of ASIC1a in the effects of GMQ. GMQ is positively charged, and the GMQ binding site in ASIC3 likely contains negatively charged amino acid residues (13). Another important electronegative region in ASICs is the "acidic pocket" between the thumb and the β-ball into which the positively charged Psalmotoxin 1 binds (9, 22). A critical residue in the acidic pocket of ASIC1a, Asp-347, was mutated to Cys followed by exposure to GMQ. GMQ induced similar acidic shifts in activation and SSIN in the mutant as in WT ASIC1a (Figs. 6E and 2B).

To test whether stronger changes at these positions might affect the GMQ-induced shift of SSIN, oocytes expressing the ASIC1a mutant E79C, D347C, or E418C were exposed to the
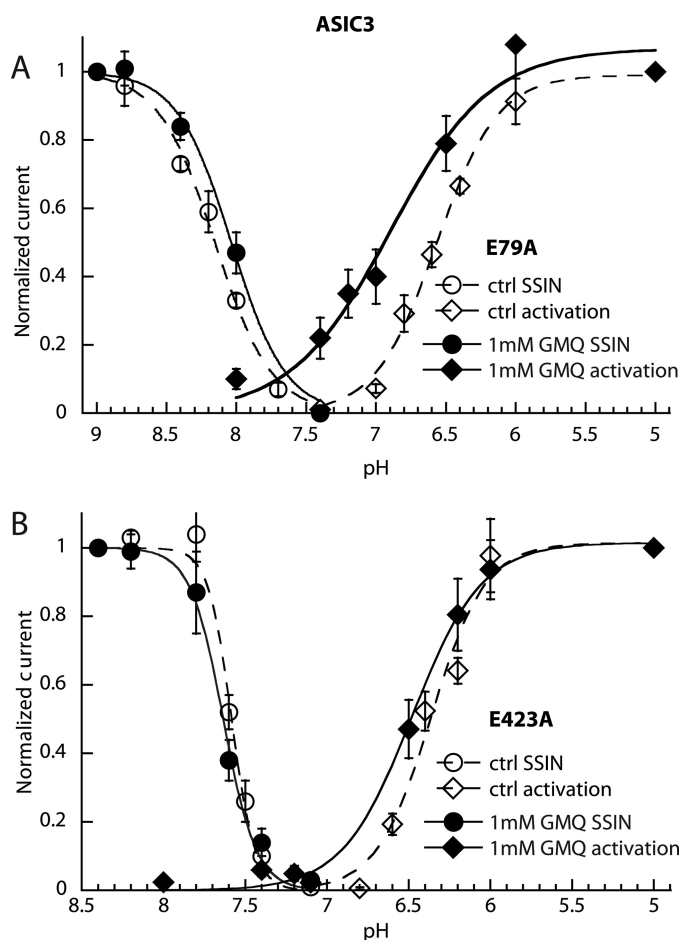
FIGURE 5. **Partial suppression of GMQ action on ASIC3 by palm mutations.** Currents were measured by whole-cell voltage clamp to −60 mV from CHO cells transfected with the mutant ASIC3 channels. SSIN curves and activation curves are shown for the mutants ASIC3-E79A (*A*) and ASIC3-E423A (*B*) in the absence (*open symbols*) or presence of 1 mM GMQ (*filled symbols*). Fit parameters are shown in supplemental Table S1 (*n* = 4–5). *Error bars* represent S.E.

sulfhydryl reagent MTSET (1 mM for 3 min), which reacts with the engineered Cys residue to produce a positively charged side chain, resulting in an opposite charge compared with the normal Asp or Glu residue at these positions. This modification induced a strong rightward shift in the SSIN curves of the mutants E79C and E418C but not the WT, indicating that MTSET had reacted with the introduced Cys residue in these mutants (compare supplemental Fig. S5, B and C, with Fig. 6, C and D). The mutant D347C is readily modified by MTSET, although this modification does not change the pH dependence of SSIN (21). Even in these MTSET-modified mutant channels, GMQ induced an acidic shift in the SSIN curve of similar amplitude as in ASIC1a WT (supplemental Fig. S5). In conclusion, these experiments indicate a role of the lower palm residues Glu-79 and Glu-418 of ASIC1a in the effects of GMQ on activation, whereas there is no evidence for such a role in the context of SSIN.

GMQ Interacts with the Amiloride Binding Site in the Pore of ASIC3—To identify potential targets of GMQ in the ASIC pore entry involved in the observed pore block, Glu-63, the two residues Glu-427 and Asp-434 predicted to mediate the pore block by divalent cations in ASIC1a (23) (Glu-432 and Asp-439 in

ASIC3), and the putative amiloride binding site Gly-440 in ASIC1a (Gly-445 in ASIC3) were individually mutated to Ala (Fig. 7*A*). Five of these eight mutants, ASIC1a-E63A, ASIC3-E63A, ASIC1a-E427A, ASIC1a-G440A, and ASIC3-G445A were functional after transfection into CHO cells. It has been shown previously that mutations in the pore region of ASICs can disrupt channel function (20, 24). We determined the pH dependence of activation of these mutants in the absence and presence of 1 mM GMQ. In addition, the inhibition of the maximal peak current amplitude by 4 mM GMQ was determined (Fig. 7). The mutation of the putative amiloride binding site induced a 2-pH unit acidic shift of the activation curve in both ASIC1a and ASIC3. GMQ changed the activation curve of all pore mutants. However, the effects of GMQ on the mutants ASIC1a-E427A and ASIC3-G445A were small (Fig. 7, *B–F*, and supplemental Tables S1 and S2). The strong shift in pH dependence induced by mutation of the amiloride binding site illustrates the reciprocal dependence between the pore region and the channel gating machinery. The reduction of the gating effects of GMQ by the ASIC3-G445A mutation indicates an involvement of this residue in the modulation of ASIC pH dependence by GMQ.

The mutation ASIC3-G445A was the only one to affect the inhibition of maximal ASIC peak currents by GMQ. At 4 mM, GMQ inhibited WT ASIC3 by 47 ± 3% and ASIC3-G445A by 31 ± 4% (Fig. 7*G*). The mutants ASIC1a-G440A and ASIC3-G445A were resistant to block by 100 μM amiloride (Fig. 7*G*). This indicates that the GMQ blocking site in ASIC3 overlaps with the amiloride binding site for channel block.

Indications on the GMQ Binding Site for the Effects on Gating in ASIC1a—Because GMQ shifts the SSIN curve of ASIC1a to more acidic pH (Fig. 2*B*), its application to channels under pH conditions in the range of the steep part of the SSIN curve (*e.g.* pH range 7.0–7.2 for ASIC1a; see Fig. 2*B*) should allow them to exit from the inactivated state. However, this can only happen if the binding site is accessible in the inactivated state. Whether this is indeed the case was tested by exposing ASIC1a-expressing cells for 40 s to pH 7.0 to inactivate the channels (this time lapse was sufficient to completely inactivate the channels; data not shown) followed first by switching for increasing durations (1–128 s) to a pH 7.0 solution containing 1 mM GMQ and then second by a step to pH 6 to determine the fraction of channels available for opening. The protocol is schematically shown in Fig. 8*A*, *upper panel*. The current amplitude measured in the test stimulus (I_2) normalized to the previously recorded reference amplitude (I_1) is plotted in Fig. 8*A* as a function of the duration of the exposure to 1 mM GMQ at pH 7.0. Current traces from a typical experiment are shown in Fig. 8*B*. The data demonstrate that GMQ can indeed make the channels recover from inactivation, demonstrating that its binding site is accessible in inactivated ASIC1a. At pH 7.0, channels recover to maximally ~80% with a rate constant of 0.042 ± 0.007 s⁻¹ (*n* = 5), which is comparable with the recovery time course at pH 7.4 in the absence of GMQ (25).

For ASIC3 activation, it had been shown that the EC$_{50}$ value for GMQ increased with increasing Ca²⁺ concentration, indicating a competition between GMQ and Ca²⁺ (13). In ASIC1a, GMQ shares several functions with Ca²⁺: similarly to Ca²⁺,
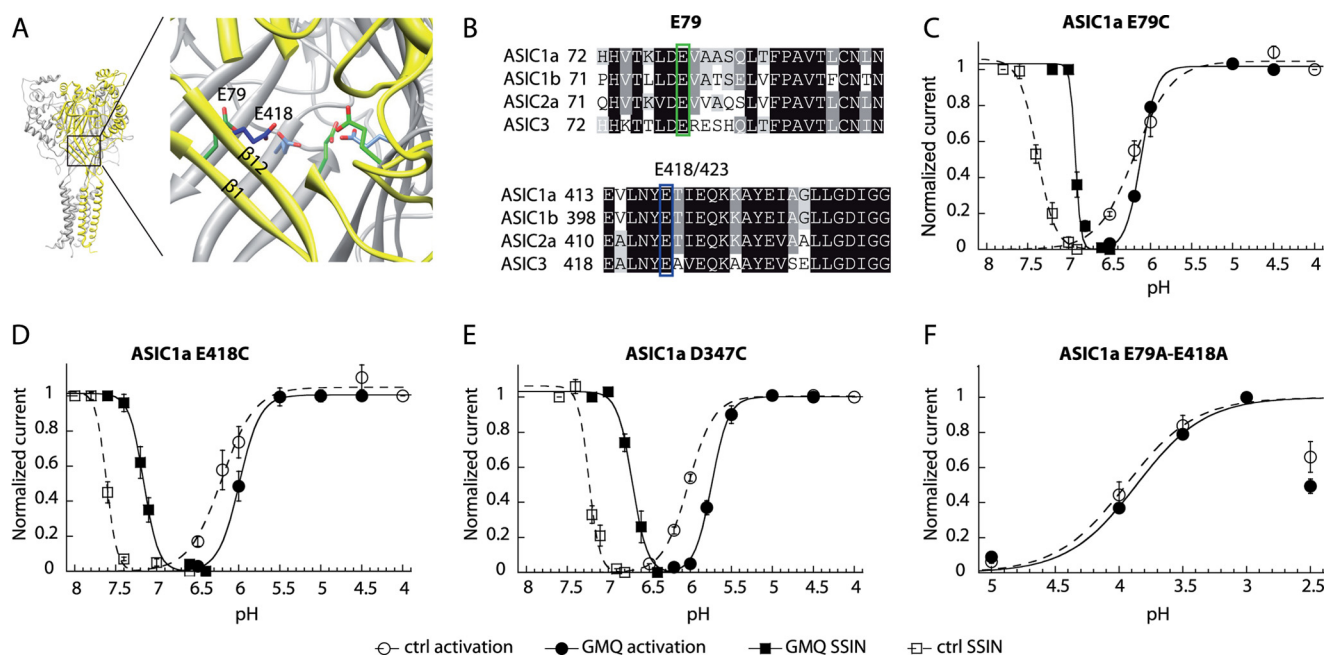
FIGURE 6. **Mutations in the lower pore domain of ASIC1a impair the gating effect of GMQ only partially.** *A*, structural model, based on the chicken ASIC1 structure, illustrating the location of residues Glu-79 in ASIC1a (*green*) and Glu-418 in ASIC1a (*blue*). Parts of the upper two β-strands of the palm in the subunit shown in *yellow* are removed to show the residues of interest. *B*, alignment of the β-strands β1 and β12 of the lower palm domains of ASIC1a, -1b, -2a, and -3. The proposed GMQ binding site residues in ASIC3, Glu-79 and Glu-423, corresponding to Glu-79 and Glu-418 in ASIC1a, are highlighted. *C–F*, currents were measured by two-electrode voltage clamp at -60 mV from *Xenopus* oocytes expressing the ASIC1a constructs. Activation and SSIN curves are shown for different ASIC1a mutants in the absence (*open symbols*) or presence of 1 mM GMQ (*filled symbols*). Data are shown for ASIC1a-E79C (C), ASIC1a-E418C (D), and ASIC1a-D347C (*E*). *F*, activation curves of the double mutant ASIC1a-E79A/E418A. The current amplitude decreased at pH 2.5; these values were not used for the fit. The pH_{50} and $pHIn_{50}$ values, obtained from the fits to individual experiments, are indicated in supplemental Table S2 ($n = 2$–10). *Error bars* represent S.E.

increasing the GMQ concentration induces acidic shifts of the pH_{50} and $pHIn_{50}$ values and reduces the unitary current amplitude (23, 26). To test whether Ca^{2+} and GMQ may compete for the same binding site(s) in ASIC1a, the shift in pH_{50} at increasing GMQ concentrations was measured in the presence of 0.1 mM extracellular Ca^{2+} (Fig. 8C) in addition to similar measurements previously carried out with 2 mM extracellular Ca^{2+} (Fig. 3A). In Fig. 8D, the GMQ concentration dependence of the shift of the pH_{50} values is compared between the two Ca^{2+} concentrations tested. The EC_{50} value of GMQ obtained in the presence of 0.1 mM Ca^{2+} was 2.17 ± 0.17 mM ($n = 4$–6), which was not lower than that obtained in the presence of 2 mM Ca^{2+} (1.90 ± 0.36 mM), indicating that there is no competition between GMQ and Ca^{2+}. This suggests that in the context of their effect on ASIC pH dependence Ca^{2+} and GMQ most likely do not bind to the same sites. In the absence of a clear molecular identity of the GMQ binding site for gating effects in ASIC1a, these experiments indicate that this site is accessible in the inactivated state and that it is not shared by Ca^{2+}.

DISCUSSION

The small molecule GMQ has been reported as an ASIC3-specific activator. In this study, we show that GMQ alters the pH dependence of all ASIC subtypes studied. However, GMQ induces a window current at pH 7.4 only in ASIC3. At concentrations >1 mM, GMQ decreases the maximal peak current amplitude by a mechanism that involves the reduction of the unitary current amplitude. Mutation of the conserved amiloride binding site in the pore of ASIC3 partially prevents the pore block by GMQ. Mutational analysis confirms the pre-

viously shown importance of the lower palm domain for the actions of GMQ and suggests that Glu-79 of the palm is not part of the binding site of GMQ but is involved in the events that follow GMQ binding.

Location of the GMQ Binding Site for Gating Effects in ASICs— It has been shown that the effect of GMQ on ASIC3 is strongly linked to residues Glu-79 and Glu-423 and several other residues in the lower palm domain of ASIC3 because mutation of these residues affected the amplitude and EC_{50} of the current increase (13, 14). It is well known that EC_{50} values depend on both the binding interaction and the subsequent steps that lead to channel opening (27). Therefore, the changes in EC_{50} do not prove that the lower palm of ASIC3 is the GMQ binding site. Our mutagenesis data of ASIC3 confirm an important role of Glu-79 and Glu-423 in the effect of GMQ. Of the mutations of homologous residues in ASIC1a, mutation E418C did not affect functional modulation by GMQ, whereas the E79C mutation prevented the GMQ-induced acidic shift of the activation curve. A change of the EC_{50} for GMQ would have been readily detected as a difference in the induced shift in the experiments with ASIC1a and on the activation of ASIC3-E79C because these experiments were carried out with GMQ concentrations close to the EC_{50} or IC_{50} values of the WT channels. The observations that mutation of ASIC3 Glu-79 prevents the action of GMQ on SSIN but not activation and that the homologous mutation in ASIC1a prevents the action of GMQ on activation but not SSIN indicate that in both cases GMQ still binds to the channel but that the functional consequences of the binding are changed.
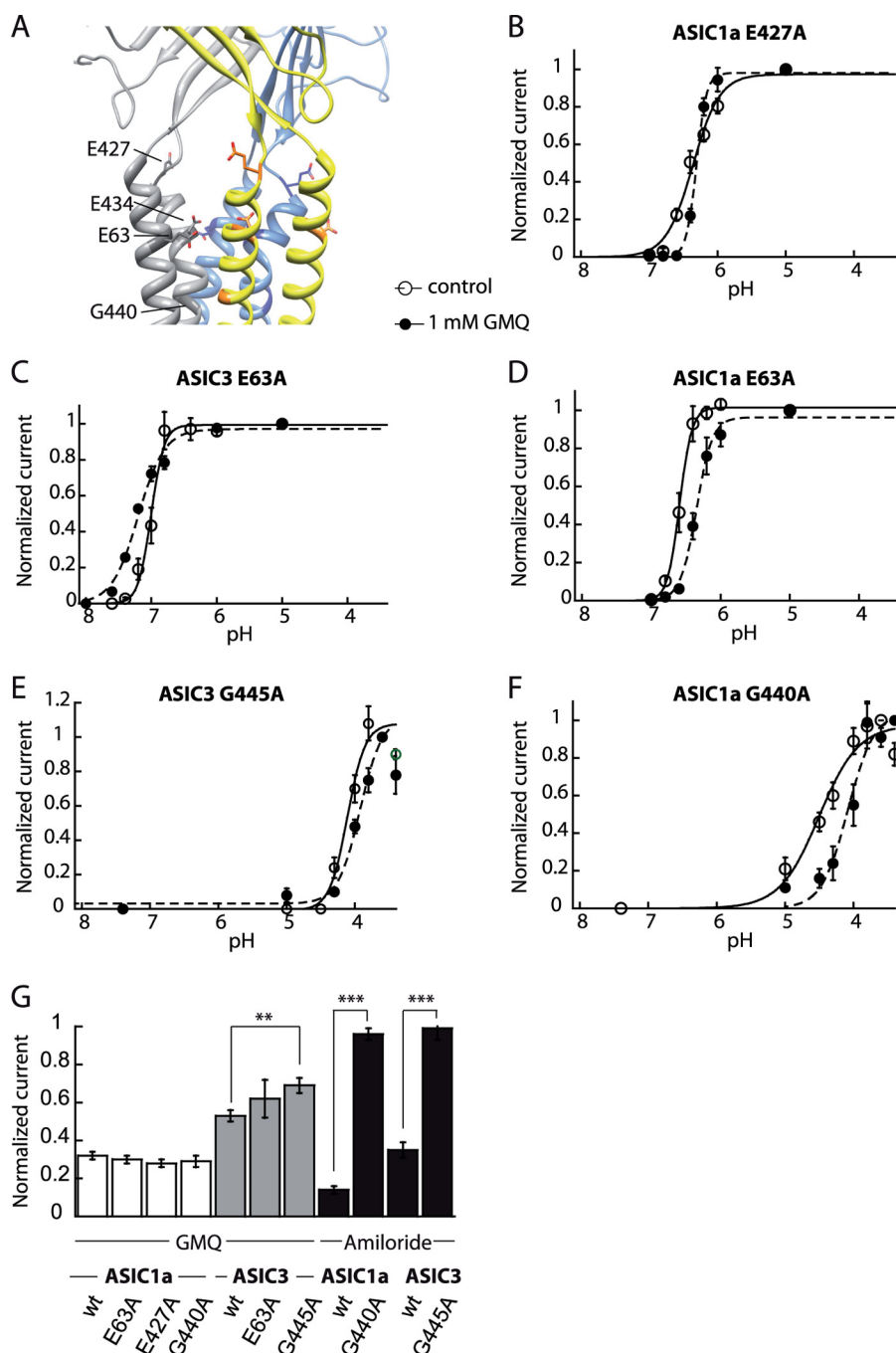
FIGURE 7. **Mutation of the conserved amiloride binding site in ASIC3 impairs pore block by GMQ.** *A*, structural model of human ASIC1a, based on the chicken ASIC1 structure, illustrating the location of potential GMQ binding residues in the outer pore domain that were mutated. *B–G*, the currents were measured by whole-cell voltage clamp to −60 mV from CHO cells expressing the indicated mutants of ASIC1a or ASIC3. *B–E*, activation curves obtained in the absence (*open symbols*) or presence of 1 mM GMQ (*filled symbols*). *B*, ASIC1a-E427A; *C*, ASIC3-E63A; *D*, ASIC1a-E63A; *E*, ASIC3-G445A; *F*, ASIC1a-G440A. *G*, bar graph presenting the inhibition of ASIC current amplitudes by 4 mM GMQ or 100 μM amiloride at acidic pH expressed as the current (in the presence of 4 mM GMQ or 100 μM amiloride)/control current ($n = 3$–9). **, different from WT, $p < 0.01$; ***, different from WT, $p < 0.001$. *Error bars* represent S.E.

Given the fact that GMQ induces an acidic shift of SSIN in all ASIC subtypes and that it has a similar potency in both ASIC3 and ASIC1a, it seems unlikely that it binds for its effects on gating to completely different sites in ASIC3 compared with the other ASIC subtypes. Our observation that GMQ could induce a recovery from inactivation in ASIC1a indicates that the GMQ binding site is accessible for GMQ in the inactivated channel. Interestingly, it has been shown previously that in ASIC3 residue Glu-79 is accessible to small methanethiosulfonate

reagents in the closed, but not the inactivated, state (20). We have observed in ASIC1a a narrowing of the central cavity to which Glu-79 and Glu-418 point during inactivation (21). These observations favor the interpretation that Glu-79 is not part of the GMQ binding site. To exert its effects on channel gating, GMQ may therefore bind in both ASIC1a and ASIC3 to a similar site to which residue Glu-79 likely does not contribute. GMQ and its analogs are considered as Arg derivatives. ASIC function is regulated by Arg-containing peptides such as FMR-
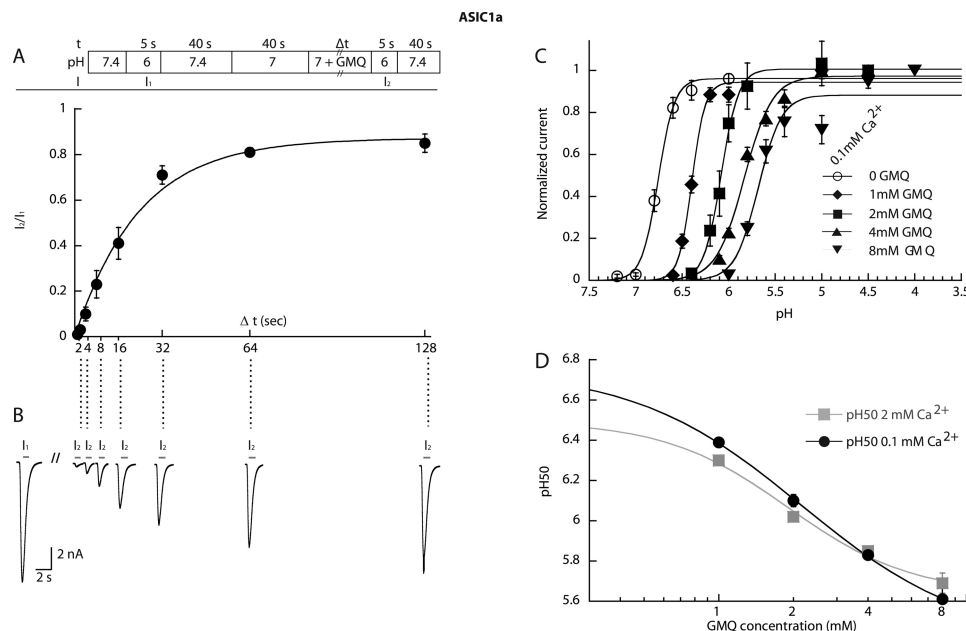
FIGURE 8. **Properties of GMQ binding for gating effects in ASIC1a.** The currents were measured by whole-cell voltage clamp to -60 mV from CHO cells stably expressing ASIC1a. *A, upper panel*, schematic view of the experimental recovery protocol; *lower panel*, the recovered current fraction (I_2/I_1 in the scheme) is plotted as a function of the duration of the exposure to 1 mM GMQ, pH 7.0 ($n = 5$). *B*, current traces of a representative recovery experiment. *C*, activation curves for ASIC1a obtained in the presence of the indicated GMQ concentrations with 0.1 mM Ca^{2+} in the stimulation solution. The *lines* represent fits to the Hill equation. *D*, pH_{50} values of experiments of *A* (0.1 mM Ca^{2+} condition) and Fig. 3*A* (2 mM Ca^{2+} condition) are plotted as a function of the GMQ concentration. Because of the logarithmic axis, pH_{50} values in the absence of GMQ are not shown. They were 6.75 ± 0.02 (0.1 mM Ca^{2+}) and 6.49 ± 0.02 (2 mM Ca^{2+}). The EC_{50} values of the GMQ-induced shift in pH_{50}, obtained from the fits shown as *solid lines*, were 2.16 ± 0.17 mM ($n = 8–6$) for 2 mM Ca^{2+} (*gray squares*) and 1.90 ± 0.36 mM ($n = 5–6$) for 0.1 mM Ca^{2+} (*filled circles*). Error bars represent S.E.

Famide and FRRFamide that add a sustained component to the H^+-induced current in ASIC1 and -3 and shift their SSIN to more acidic pH but do not activate these channels (28). Currently, the binding site of these peptides is not known. The two peptide toxins that inhibit ASICs, Psalmotoxin 1 and APETx2, both contain Arg residues that are important for their function (29, 30). Psalmotoxin 1 was shown to bind into the acidic pocket between the thumb and the palm domain (22). Psalmotoxin1 inhibits ASICs by shifting the pH dependence of SSIN to more alkaline values, thus in the opposite direction of GMQ (31).

GMQ Is a Pore Blocker of ASICs—GMQ at concentrations >1 mM induced in all ASIC subtypes tested an inhibition of the maximal peak currents. Except for ASIC1b, this inhibition was small at 1 mM GMQ. At this concentration, GMQ changed the pH dependence substantially and significantly. The shifted concentration dependence between the inhibition of the maximal peak current and the changes in pH dependence suggested that they may be mediated by different binding sites similarly to what has been proposed for Ca^{2+} on ASIC1a (23, 26). We show for ASIC1a and ASIC3 that the inhibition by GMQ is due to a reduction in unitary current amplitude. We found that mutation of the conserved amiloride binding site in ASIC3 decreased the inhibition by GMQ. Together, this strongly suggests that the inhibitory site is located in the pore and overlaps with the amiloride binding site. The observation that mutation of the amiloride binding site of ASIC1a did not affect the inhibition of the maximal peak current by GMQ indicates that other pore residues likely also contribute to the GMQ blocking site.

ASIC Subtype-specific Effect of GMQ—We confirmed that 1 mM GMQ opens ASIC3 at pH 7.4 as shown previously (13). We demonstrate that GMQ does so by affecting SSIN and activa-

tion: it shifts the SSIN curve to more acidic pH and the activation curve to more alkaline pH and renders both curves less steep. In this way, it induces a window current at pH 7.4. GMQ shifts the SSIN curve to more acidic pH in all ASIC subtypes tested. In ASIC1a and -1b, GMQ shifts the pH dependence of activation to more acidic pH, thus in the opposite direction than in ASIC3. In a physiological setting, GMQ and likely the endogenous analog agmatine will tend to decrease ASIC1a- and ASIC1b-mediated currents due to the acidic shift in activation pH dependence. It will also open ASIC3 at pH 7.4 and potentiate the proton-induced ASIC3 currents. This explains the strong dependence on ASIC3 for the induction of pain-related behavior by GMQ and agmatine (13, 32).

In our study, the relative amplitude of the ASIC3 current induced by 1 mM GMQ at pH 7.4 was smaller than that reported previously. The EC_{50} of GMQ on ASIC3 was ~2 mM in our experiments compared with ~1 mM reported previously (13). The purity of our GMQ preparation was 98% (see "Experimental "Procedures"). The observed differences might be due to different experimental conditions or differences in the ASIC3 clones used.

Potential Mechanisms Underlying the Subtype Specificity of the Effects of GMQ—In ASIC3, the mechanism of channel opening might be quite different from that of other ASICs. Based on the observation that a strong reduction in extracellular Ca^{2+} can open ASIC3 at pH 7.4, it was suggested that protons open the channel by displacing Ca^{2+} from a pore blocking site (33). Such an effect of Ca^{2+} is not found in ASIC1a (23, 34). Differences in fundamental mechanisms of channel opening may be the cause of the opposite effects of GMQ on the pH dependence of activation of ASIC1a and ASIC3. ASIC3 is dif-

ferent from the other ASICs in an additional way as it mediates a sustained current component at very acidic pH (*i.e.* at pH <5) (18). It also shows a small sustained current at pH ~7 (19) (Fig. 1, *A* and *C*). GMQ may uncover the inherent property of ASIC3 in mediating a sustained current at physiological pH that is normally only possible in other pH ranges. The available data do not allow distinguishing between two different possibilities that 1) GMQ shifts the pH dependence of the normal ASIC open state to induce the observed window current or 2) GMQ creates a new open state in addition to the normal opening similar to what has been proposed for the degenerin site in ASIC2a (35). Our observation that the GMQ-induced current is inhibited by amiloride with an IC_{50} similar to that of the transient control current may favor the first interpretation. However, the shift in the pH dependence occurs exactly in the pH range with the highest amplitude of sustained current. Structural elements involved in the generation of the sustained current of ASIC3 are intracellular and transmembrane domains (36) to which the charged GMQ, whose effects are rapidly reversible, likely does not bind. In ASIC1a, mutations in the palm region were shown to produce sustained currents (37). It was recently shown that amiloride opens ASIC3 at high concentrations in a similar way to GMQ (17) (supplemental Fig. S1). Interestingly, it has been suggested previously that amiloride or related substances may induce an active conformation in ASIC2a and epithelial sodium channel, probably by binding to a different site than the pore blocking site (38–40).

In conclusion, this study demonstrates that GMQ alters the pH dependence of ASIC gating in all functional homomultimeric ASICs. In ASIC3, this allows GMQ to open the channels at pH 7.4. The underlying mechanisms of these subtype-specific effects of GMQ may be linked to inherent differences in the fundamental principles of gating between ASIC3 and other ASICs.

REFERENCES

1. Kellenberger, S., and Schild, L. (2002) Epithelial sodium channel/degenerin family of ion channels: a variety of functions for a shared structure. *Physiol. Rev.* **82,** 735–767
2. Wemmie, J. A., Price, M. P., and Welsh, M. J. (2006) Acid-sensing ion channels: advances, questions and therapeutic opportunities. *Trends Neurosci.* **29,** 578–586
3. Xiong, Z. G., Zhu, X. M., Chu, X. P., Minami, M., Hey, J., Wei, W. L., MacDonald, J. F., Wemmie, J. A., Price, M. P., Welsh, M. J., and Simon, R. P. (2004) Neuroprotection in ischemia: blocking calcium-permeable acid-sensing ion channels. *Cell* **118,** 687–698
4. Ziemann, A. E., Allen, J. E., Dahdaleh, N. S., Drebot, I. I., Coryell, M. W., Wunsch, A. M., Lynch, C. M., Faraci, F. M., Howard, M. A., 3rd, Welsh, M. J., and Wemmie, J. A. (2009) The amygdala is a chemosensor that detects carbon dioxide and acidosis to elicit fear behavior. *Cell* **139,** 1012–1021
5. Wemmie, J. A., Chen, J., Askwith, C. C., Hruska-Hageman, A. M., Price, M. P., Nolan, B. C., Yoder, P. G., Lamani, E., Hoshi, T., Freeman, J. H., Jr., and Welsh, M. J. (2002) The acid-activated ion channel ASIC contributes to synaptic plasticity, learning, and memory. *Neuron* **34,** 463–477
6. Price, M. P., McIlwrath, S. L., Xie, J., Cheng, C., Qiao, J., Tarr, D. E., Sluka, K. A., Brennan, T. J., Lewin, G. R., and Welsh, M. J. (2001) The DRASIC cation channel contributes to the detection of cutaneous touch and acid stimuli in mice. *Neuron* **32,** 1071–1083
7. Lu, Y., Ma, X., Sabharwal, R., Snitsarev, V., Morgan, D., Rahmouni, K., Drummond, H. A., Whiteis, C. A., Costa, V., Price, M., Benson, C., Welsh, M. J., Chapleau, M. W., and Abboud, F. M. (2009) The ion channel ASIC2 is required for baroreceptor and autonomic control of the circulation. *Neuron* **64,** 885–897
8. Deval, E., Noël, J., Lay, N., Alloui, A., Diochot, S., Friend, V., Jodar, M., Lazdunski, M., and Lingueglia, E. (2008) ASIC3, a sensor of acidic and primary inflammatory pain. *EMBO J.* **27,** 3047–3055
9. Jasti, J., Furukawa, H., Gonzales, E. B., and Gouaux, E. (2007) Structure of acid-sensing ion channel 1 at 1.9 Å resolution and low pH. *Nature* **449,** 316–323
10. Gonzales, E. B., Kawate, T., and Gouaux, E. (2009) Pore architecture and ion sites in acid-sensing ion channels and P2X receptors. *Nature* **460,** 599–604
11. Lingueglia, E., de Weille, J. R., Bassilana, F., Heurteaux, C., Sakai, H., Waldmann, R., and Lazdunski, M. (1997) A modulatory subunit of acid sensing ion channels in brain and dorsal root ganglion cells. *J. Biol. Chem.* **272,** 29778–29783
12. Donier, E., Rugiero, F., Jacob, C., and Wood, J. N. (2008) Regulation of ASIC activity by ASIC4—new insights into ASIC channel function revealed by a yeast two-hybrid assay. *Eur. J. Neurosci.* **28,** 74–86
13. Yu, Y., Chen, Z., Li, W. G., Cao, H., Feng, E. G., Yu, F., Liu, H., Jiang, H., and Xu, T. L. (2010) A nonproton ligand sensor in the acid-sensing ion channel. *Neuron* **68,** 61–72
14. Yu, Y., Li, W. G., Chen, Z., Cao, H., Yang, H., Jiang, H., and Xu, T. L. (2011) Atomic level characterization of the nonproton ligand-sensing domain of ASIC3 channels. *J. Biol. Chem.* **286,** 24996–25006
15. García-Añoveros, J., Derfler, B., Neville-Golden, J., Hyman, B. T., and Corey, D. P. (1997) BNaC1 and BNaC2 constitute a new family of human neuronal sodium channels related to degenerins and epithelial sodium channels. *Proc. Natl. Acad. Sci. U.S.A.* **94,** 1459–1464
16. Poirot, O., Berta, T., Decosterd, I., and Kellenberger, S. (2006) Distinct ASIC currents are expressed in rat putative nociceptors and are modulated by nerve injury. *J. Physiol.* **576,** 215–234
17. Li, W. G., Yu, Y., Huang, C., Cao, H., and Xu, T. L. (2011) The nonproton ligand sensing domain is required for paradoxical stimulation of ASIC3 channels by amiloride. *J. Biol. Chem.* **286,** 42635–42646
18. Waldmann, R., Bassilana, F., de Weille, J., Champigny, G., Heurteaux, C., and Lazdunski, M. (1997) Molecular cloning of a non-inactivating proton-gated Na^+ channel specific for sensory neurons. *J. Biol. Chem.* **272,** 20975–20978
19. Yagi, J., Wenk, H. N., Naves, L. A., and McCleskey, E. W. (2006) Sustained currents through ASIC3 ion channels at the modest pH changes that occur during myocardial ischemia. *Circ. Res.* **99,** 501–509
20. Cushman, K. A., Marsh-Haffner, J., Adelman, J. P., and McCleskey, E. W. (2007) A conformation change in the extracellular domain that accompanies desensitization of acid-sensing ion channel (ASIC) 3. *J. Gen. Physiol.* **129,** 345–350
21. Liechti, L. A., Bernèche, S., Bargeton, B., Iwaszkiewicz, J., Roy, S., Michielin, O., and Kellenberger, S. (2010) A combined computational and functional approach identifies new residues involved in pH-dependent gating of ASIC1a. *J. Biol. Chem.* **285,** 16315–16329
22. Dawson, R. J., Benz, J., Stohler, P., Tetaz, T., Joseph, C., Huber, S., Schmid, G., Hügin, D., Pflimlin, P., Trube, G., Rudolph, M. G., Hennig, M., and Ruf, A. (2012) Structure of the Acid-sensing ion channel 1 in complex with the gating modifier Psalmotoxin 1. *Nat. Commun.* **3,** 936
23. Paukert, M., Babini, E., Pusch, M., and Gründer, S. (2004) Identification of the Ca^{2+} blocking site of acid-sensing ion channel (ASIC) 1: implications for channel gating. *J. Gen. Physiol.* **124,** 383–394
24. Li, T., Yang, Y., and Canessa, C. M. (2011) Outlines of the pore in open and closed conformations describe the gating mechanism of ASIC1. *Nat. Commun.* **2,** 399
25. Blanchard, M. G., and Kellenberger, S. (2011) Effect of a temperature

increase in the non-noxious range on proton-evoked ASIC and TRPV1 activity. *Pflugers Arch.* **461,** 123–139

26. Babini, E., Paukert, M., Geisler, H. S., and Grunder, S. (2002) Alternative splicing and interaction with di- and polyvalent cations control the dynamic range of acid-sensing ion channel 1 (ASIC1). *J. Biol. Chem.* **277,** 41597–41603

27. Colquhoun, D. (1998) Binding, gating, affinity and efficacy: the interpretation of structure-activity relationships for agonists and of the effects of mutating receptors. *Br. J. Pharmacol.* **125,** 924–947

28. Sherwood, T. W., and Askwith, C. C. (2008) Endogenous arginine-phenylalanine-amide-related peptides alter steady-state desensitization of ASIC1a. *J. Biol. Chem.* **283,** 1818–1830

29. Diochot, S., Baron, A., Rash, L. D., Deval, E., Escoubas, P., Scarzello, S., Salinas, M., and Lazdunski, M. (2004) A new sea anemone peptide, APETx2, inhibits ASIC3, a major acid-sensitive channel in sensory neurons. *EMBO J.* **23,** 1516–1525

30. Escoubas, P., De Weille, J. R., Lecoq, A., Diochot, S., Waldmann, R., Champigny, G., Moinier, D., Ménez, A., and Lazdunski, M. (2000) Isolation of a tarantula toxin specific for a class of proton-gated Na$^+$ channels. *J. Biol. Chem.* **275,** 25116–25121

31. Chen, X., Kalbacher, H., and Gründer, S. (2005) The tarantula toxin Psalmotoxin 1 inhibits acid-sensing ion channel (ASIC) 1a by increasing its apparent H$^+$ affinity. *J. Gen. Physiol.* **126,** 71–79

32. Li, W. G., Yu, Y., Zhang, Z. D., Cao, H., and Xu, T. L. (2010) ASIC3 channels integrate agmatine and multiple inflammatory signals through the nonproton ligand sensing domain. *Mol. Pain* **6,** 88

33. Immke, D. C., and McCleskey, E. W. (2003) Protons open acid-sensing ion channels by catalyzing relief of Ca^{2+} blockade. *Neuron* **37,** 75–84

34. Zhang, P., Sigworth, F. J., and Canessa, C. M. (2006) Gating of acid-sensitive ion channel-1: release of Ca^{2+} block *vs.* allosteric mechanism. *J. Gen. Physiol.* **127,** 109–117

35. Champigny, G., Voilley, N., Waldmann, R., and Lazdunski, M. (1998) Mutations causing neurodegeneration in *Caenorhabditis elegans* drastically alter the pH sensitivity and inactivation of the mammalian H$^+$-gated Na$^+$ channel MDEG1. *J. Biol. Chem.* **273,** 15418–15422

36. Salinas, M., Lazdunski, M., and Lingueglia, E. (2009) Structural elements for the generation of sustained currents by the acid pain sensor ASIC3. *J. Biol. Chem.* **284,** 31851–31859

37. Springauf, A., Bresenitz, P., and Grunder, S. (2011) The interaction between two extracellular linker regions controls sustained opening of acid-sensing ion channel 1. *J. Biol. Chem.* **286,** 24374–24384

38. Horisberger, J. D., and Chraïbi, A. (2004) Epithelial sodium channel: a ligand-gated channel? *Nephron Physiol.* **96,** p37–41

39. Lu, M., Echeverri, F., Kalabat, D., Laita, B., Dahan, D. S., Smith, R. D., Xu, H., Staszewski, L., Yamamoto, J., Ling, J., Hwang, N., Kimmich, R., Li, P., Patron, E., Keung, W., Patron, A., and Moyer, B. D. (2008) Small molecule activator of the human epithelial sodium channel. *J. Biol. Chem.* **283,** 11981–11994

40. Adams, C. M., Snyder, P. M., and Welsh, M. J. (1999) Paradoxical stimulation of a DEG/ENaC channel by amiloride. *J. Biol. Chem.* **274,** 15500–15504